



This is the accepted manuscript made available via CHORUS, the article has been published as:

Spin Liquids and Antiferromagnetic Order in the Shastry-Sutherland-Lattice Compound $\text{Yb}_2\text{Pt}_2\text{Pb}$

M. S. Kim and M. C. Aronson

Phys. Rev. Lett. **110**, 017201 — Published 2 January 2013

DOI: [10.1103/PhysRevLett.110.017201](https://doi.org/10.1103/PhysRevLett.110.017201)

Spin Liquids and Antiferromagnetic Order in the Shastry-Sutherland-Lattice $\text{Yb}_2\text{Pt}_2\text{Pb}$

M. S. Kim

Department of Physics and Astronomy, Stony Brook University, Stony Brook NY 11794, USA

M. C. Aronson

*Brookhaven National Laboratory, Upton, New York 11973, USA and
Department of Physics and Astronomy, Stony Brook University, Stony Brook NY 11794, USA*

We present measurements of the magnetic susceptibility χ and the magnetization M of single crystals of metallic $\text{Yb}_2\text{Pt}_2\text{Pb}$, where localized Yb moments lie on the dimerized and frustrated Shastry-Sutherland Lattice (SSL). Strong magnetic frustration is found in this quasi-two dimensional system, which orders antiferromagnetically (AF) at $T_N=2.02\text{ K}$ from a paramagnetic liquid of Yb-dimers, having a gap $\Delta=4.6\text{ K}$ between the singlet ground state and the triplet excited states. Magnetic fields suppress the AF order, which vanishes at a 1.23 T quantum critical point. The spin gap Δ persists to 1.5 T , indicating that dimer singlets survive the collapse of the $B=0$ AF state. Quantized steps are observed in $M(B)$ within the AF state, a signature of SSL systems. Our results show that $\text{Yb}_2\text{Pt}_2\text{Pb}$ is unique, both as a metallic SSL system that is close to an AF quantum critical point, and as a heavy fermion compound where quantum frustration plays a decisive role.

PACS numbers: 75.10.Kt, 75.20.Hr, 75.30.Kz

Much interest has focused on systems with quantum frustration, where conventional antiferromagnetic (AF) order is suppressed in favor of more exotic ground states. The Shastry Sutherland Lattice (SSL) is one of the simplest frustrated systems [1], consisting of planes of orthogonal dimers of moments with interdimer coupling J' and the intradimer coupling J . The $T=0$ phase diagram has two limiting behaviors, depending on J'/J . Nonordering dimers are found for small J'/J , distinguished by an energy gap Δ between the singlet and triplet states of the dimer. Insulating $\text{SrCu}_2(\text{BO}_3)_2$ exemplifies this disordered 'spin liquid' (SL) regime [2–4]. Conversely, AF order with gapless magnetic excitations is favored for large J'/J , and the RB_4 ($R = \text{Gd, Tb, Dy, Ho, Er}$) compounds may represent this limit [5–8]. A $T=0$ transition between the SL and AF phases has been predicted for $J'/J \simeq 0.6 - 0.7$ [3, 9–11], although symmetry-based arguments [12] suggest that an intermediate state is required, such as a helical magnet [13], a weak SDW [12], or a plaquet ordered solid [14]. The known SSL systems have so far not provided experimental access to this transitional regime.

Metallic SSL systems have the potential for a more complex $T=0$ phase diagram, especially those based on Ce and Yb where the doublet ground state crucial for dimer formation may be realized. Here, the hybridization of f-electrons with conduction electrons can result in Kondo physics and electronic delocalization, central to heavy fermion (HF) compounds. A universal $T=0$ phase diagram has been proposed for HFs [15, 16]. The first axis represent increasing quantum fluctuations, introduced via geometrical frustration or dimerization as in the SSL, which suppress magnetic order above a critical value [17–20]. No electronic delocalization is associated with this frustration driven quantum critical point (QCP). The second axis is realized in unfrustrated HFs,

where increasing hybridization between the f-electrons and conduction electrons suppresses magnetic order at a second QCP [21–23].

By including the possibility of electronic delocalization, both ordered and paramagnetic phases are further divided into sub-phases where the f-electrons are localized or excluded from the Fermi surface and those where the f-electrons are delocalized and included in the Fermi surface. Experiments on unfrustrated HFs have provided support for this phase diagram [24–28], however the discovery of Ce and Yb based SSL systems may enable the first exploration of the region of this phase diagram where quantum fluctuations are decisive. Several metallic SSL systems are already known. Complex magnetic order is found in $\text{Ce}_2\text{Pd}_2\text{Sn}$, where novel low temperature properties arise from ferromagnetic (FM) dimers with the $S=1$ ground state [29]. Nonordering $\text{Yb}_2\text{Pd}_2\text{Sn}$ can be driven AF via pressure [30] and In doping [31], but the $T_K=17\text{ K}$ of $\text{Yb}_2\text{Pd}_2\text{Sn}$ remains large throughout. No evidence for dimer formation, such as a singlet-triplet gap, is found and instead the magnetic susceptibility χ becomes constant as $T \rightarrow 0$, indicating that Kondo physics dominates in $\text{Yb}_2\text{Pd}_2\text{Sn}$ [20]. In contrast, $\text{Yb}_2\text{Pt}_2\text{Pb}$ orders antiferromagnetically at $T_N=2.02\text{ K}$, and the role of Kondo physics in the paramagnetic state remains unclear.

We argue here that $\text{Yb}_2\text{Pt}_2\text{Pb}$ is a SSL system where both frustration and Kondo physics are important. Dimer formation characteristic of the SSL is evidenced in $\text{Yb}_2\text{Pt}_2\text{Pb}$ by a broad maximum in the magnetic susceptibility $\chi(T)$, suggesting that AF order emerges from a dimer fluid with a singlet-triplet gap Δ . Magnetic fields suppress the $B=0$ AF order more quickly than the spin gap Δ , indicating that a SL of singlet and triplet dimers persists at higher fields and may provide a driving force for subsequent ordered phases. Quantized magnetization steps are a signature of other SSL systems, such

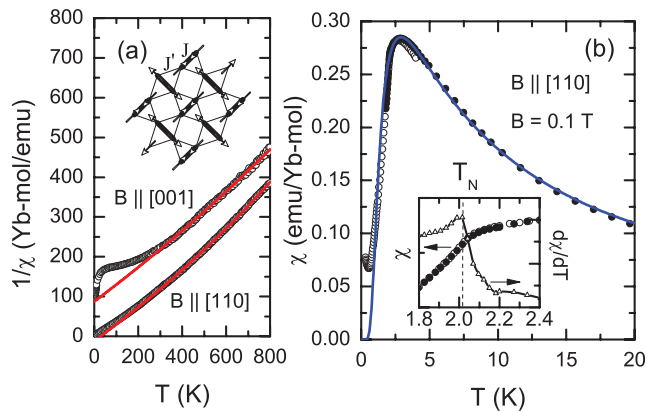


FIG. 1: (Color online) (a) Temperature dependencies of $1/\chi$ for fixed fields $B=2 \text{ T}$ ($T \geq 300 \text{ K}$) and $B=0.1 \text{ T}$ ($T \leq 300 \text{ K}$) along $[001]$ and $[110]$, after [32]. Solid red lines are fits to Curie-Weiss expressions for $T \geq 200 \text{ K}$. Inset: the Shastry-Sutherland lattice has interdimer J' and intradimer J couplings as indicated, with moments directed along the dimer bonds. (b) $\chi(T)=M/B$ for $B=0.1 \text{ T}$ (MPMS: \bullet , Hall sensor: \circ). Solid line is fit to dimer expression (see text). Inset: expanded view of region near $T_N=2.02 \text{ K}$. (vertical dashed line). χ : \bullet , \circ ; $d\chi/dT$: Δ . Solid line is a guide for the eye.

as $\text{SrCu}_2(\text{BO}_3)_2$ and the RB_4 compounds, and they are observed as well within the AF phase of $\text{Yb}_2\text{Pt}_2\text{Pb}$. As a SSL system, $\text{Yb}_2\text{Pt}_2\text{Pb}$ exemplifies a regime near AF instability that has not previously been experimentally accessible. As a potential HF, $\text{Yb}_2\text{Pt}_2\text{Pb}$ is one of the first systems where the interplay of frustration and quantum criticality can be investigated, and the modestly enhanced Sommerfeld coefficient $\gamma=30 \text{ mJ/mol K}^2$ and the slow saturation of $M(B)$ suggests there may be sufficient hybridization of the Yb^{3+} f-electrons and the conduction electrons to provide a role for Kondo physics [19, 32].

All experiments were performed on single crystals of $\text{Yb}_2\text{Pt}_2\text{Pb}$ that were prepared from Pb flux [32]. The electrical resistivity ρ of $\text{Yb}_2\text{Pt}_2\text{Pb}$ is metallic and approaches a residual value $\rho_0=1.5 \mu\Omega\text{-cm}$, attesting to low levels of crystalline disorder [32]. Measurements of the dc magnetization M were conducted at fixed fields ranging from $0.1 - 4 \text{ T}$ in a Quantum Designs Magnetic Properties Measurement System (MPMS) for temperatures from 1.8 K - 300 K , while a Hall sensor magnetometer was used for temperatures from 0.06 K - 4 K [33].

The inverse magnetic susceptibility $(\chi(T))^{-1}=(M/B)^{-1}$ (Fig. 1a) is linear for temperatures from $200 \text{ K} \leq T \leq 800 \text{ K}$, where the fluctuating moments with $B \parallel (110)$ and $B \parallel (110)$ are both close to the $4.5 \mu_B/\text{Yb}^{3+}$ expected for a fully occupied manifold of crystal field split states. The crystal field splittings are known from specific heat measurements [32], and for $20 \text{ K} \leq T \leq 80 \text{ K}$, where only the ground doublet is appreciably occupied, χ with $B \parallel (110)$ is still well described by a Curie-Weiss temperature dependence $\chi(T)=\chi_0+C/(T-\theta_{ab})$, where the fluctuating moments are still $\sim 4.5 \mu_B/\text{Yb}^{3+}$, suggestive of substantial

single ion anisotropy. A large, quasi-two dimensional anisotropy is found in $\chi(T)$ at all temperatures (Fig. 1a), indicating that the Yb moments are largely confined to the basal plane by single ion anisotropy and possibly also by interactions at the lowest temperatures where the Yb moments are directed along the (110) and equivalent easy directions (Fig. 1a, inset) [32]. A slope discontinuity in χ and the accompanying maximum in $d\chi/dT$ marks the onset of AF order at $T_N=2.02 \text{ K}$, slightly below the $T_N=2.07 \text{ K}$ that is found in specific heat measurements [32](Fig. 1b, inset). The Weiss temperature θ_{ab} is substantially larger than T_N , implying a substantial frustration figure of merit [34] $f=\theta_{ab}/T_N \simeq 4$ for $\text{Yb}_2\text{Pt}_2\text{Pb}$.

A broad peak is observed in $\chi(T)$ for $B \parallel [110]$ (Fig. 1b), indicating that the ground state of $\text{Yb}_2\text{Pt}_2\text{Pb}$ is non-magnetic. The magnetic susceptibility $\chi(T)$ ($B \parallel [110]$) is well described using the mean field expression $\chi(T)=\chi_D/(1-2nj'\chi_D)$, where $j'=k_B J'/(g\mu_B)^2$ is the dimensionless interdimer coupling, n the number of near neighbors, and χ_D is the susceptibility of a single dimer. Both of the Yb moments contribute two states, and coupling these moments into a dimer produces a singlet ground state and a triplet excited state, separated for $B=0$ by an energy $\Delta=-2J$. χ_D is readily calculated from this energy level scheme [35], taking N to be the number of dimers, k_B the Boltzmann constant, μ_B the Bohr magneton, and g the Landé g-factor: $\chi_D=(2N(g\mu_B)^2)/[k_B T(\exp(-\Delta/k_B T)+3)]$. Although there is a small upturn in $\chi(T)$ at the lowest temperatures, perhaps indicating that a few Yb moments or even stray impurity moments do not participate in the magnetic dimers, the fit (Fig. 1b) provides an excellent account of the measured $B=0.1 \text{ T}$ susceptibility $\chi(T)$ in the paramagnetic regime $T \geq T_N$ when $\Delta=4.3 \pm 0.04 \text{ K}$, $J=-2.3 \pm 0.01 \text{ K}$, $J'=-1.95 \pm 0.03 \text{ K}$, and $g=5.43 \pm 0.02$, the last consistent with observations in other systems where Yb^{3+} is in a tetragonal crystal field [36].

Magnetic fields affect both T_N and Δ , fundamentally changing the balance of phases present in $\text{Yb}_2\text{Pt}_2\text{Pb}$ at $B=0$. Increasing magnetic fields $B \parallel [110]$ shift both the slope discontinuity in $M(T_N)$ (Fig. 2a) and its associated peak in $d\chi/dB$ (Fig. 2b, inset), as well as the broad maximum in $\chi(T)$ (Fig. 2b) to lower temperatures. $T_N(B)$ is taken from the maximum in $d\chi/dT$ (inset, Fig. 1b) and the maxima in dM/dB (inset, Fig. 2b), and the values of T_N determined for each field B are shown in Fig. 3a. The inset of Fig. 3a shows that T_N vanishes for $B_{QCP}=1.23 \pm 0.01 \text{ T}$, following $T_N \sim (B_{QCP}-B)^\nu$ with the XY class exponent $\nu=0.43 \pm 0.03$ [37]. This behavior resembles that of HFs like YbRh_2Si_2 [38] and CeRhIn_5 [39] near their AF-QCPs. In contrast, the Bose Einstein Condensation (BEC) exponent $\nu=2/3$ is found in quantum magnets like $\text{BaCuSi}_2\text{O}_6$ [40] and TlCuCl_3 [41], where magnetic fields induce $T=0$ AF order by driving $\Delta \rightarrow 0$, via the Zeeman splitting of excited triplet states [42].

Δ and T_N appear to vanish at different fields in

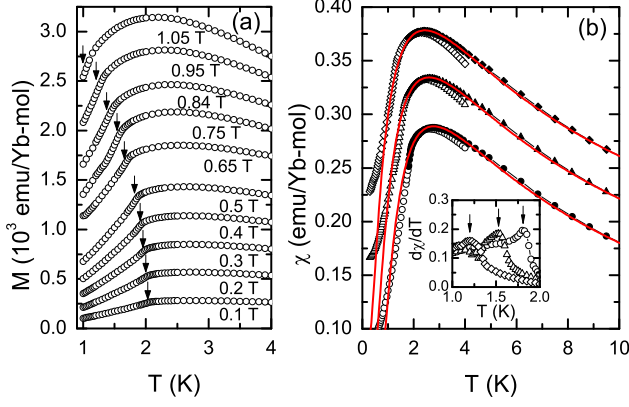


FIG. 2: (Color online)(a) Magnetization M for different fields B (indicated). Arrows mark T_N , taken from the peak in $d(M/B)/dT$. (b) $\chi(T)=M/B$ for different values of B \parallel $[110]$ (\circ : 0.5 T, \triangle : 0.75 T, \blacklozenge : 0.95 T). Solid red lines are mean field expression for χ (see text). Inset: arrows indicate peaks in $d\chi/dT$ at T_N , obtained for $B=0.5$ T, 0.75 T, and 0.95 T (right to left).

$\text{Yb}_2\text{Pt}_2\text{Pb}$. The analysis of the $B=0$ $\chi(T)$ can be generalized for $B \neq 0$, using the energy level scheme depicted in Fig. 3b (inset). Each dimer has a singlet ground state ($E_0=3/2 J$), and three excited states with energies $E_1=-1/2J-g\mu_B B$, $E_2=-1/2J$, and $E_3=-1/2J+g\mu_B B$. The dimer magnetization M_d is derived from the partition function of these four states, yielding the expression:

$$M_d = \frac{2g\mu_B \sinh(g\mu_B B/k_B T)}{1 + \exp(-2J/k_B T) + 2 \cosh(g\mu_B B/k_B T)}$$

The susceptibility χ of N interacting dimers, each with n neighbors, is given in turn by the mean field expression $\chi(B,T) = N\chi_d/(1-2J'n\chi_d)$, where the dimer susceptibility $\chi_d=dM_d/dB$. The experimental data at different fixed fields are fitted to this expression for $\chi(T)$ (Fig. 2b), and the resulting values for J , J' , and g are determined for each field. The values of the singlet and triplet energies that are calculated using these values of g and J' are plotted, forming the level scheme that is presented in the inset of Fig. 3b. The Zeeman splitting derived from this analysis gives $\Delta(B)=E_1-E_0 = -2 J-g\mu_B B$, where Δ drops almost linearly from its $B=0.1$ T value of 4.3 K to zero for $B_\Delta=1.5$ T (Fig. 3a). We deduce that $\Delta(B=0)=4.6$ K, by extrapolating the $B=0.1$ T value $\Delta=4.3$ K to $B=0$. The relative magnitudes of $J=-2.3 \pm 0.01$ K and $J' = -1.95 \pm 0.03$ K extracted from the $B=0.1$ T fit give the ratio $J'/J=0.85$, a value that is larger than the critical value $(J'/J)_C=0.6-0.7$, placing $\text{Yb}_2\text{Pt}_2\text{Pb}$ within the expected AF regime of the $S=1/2$ SSL [1].

The phase diagram that is formed by comparing the phase line $T_N(B)$ to the energy scale $\Delta(B)/k_B$ (Fig. 3a) indicates that for $B_{QCP} \leq B \leq B_\Delta$, there is a nonzero singlet triplet gap Δ . The disappearance of Δ for $B=B_\Delta$

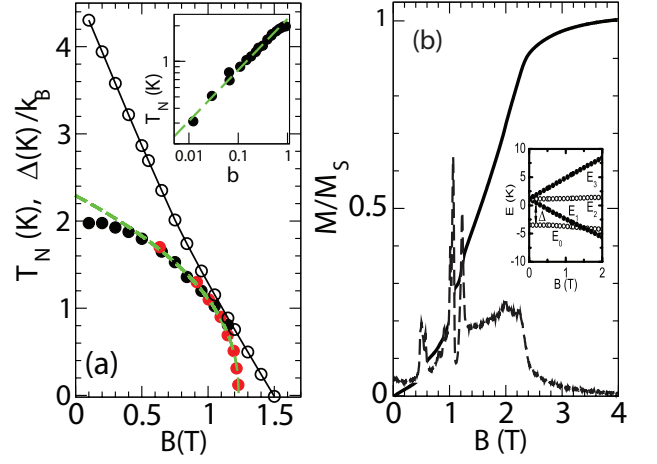


FIG. 3: (Color online) (a) The field dependencies of the Neel temperature T_N , taken from $M(T)$ (black filled circles) and $M(B)$ (red filled circles, example of raw data shown in Fig. 3b) sweeps and the singlet-triplet dimer gap Δ (open circles). Green dashed line is the fit to $T_N \simeq (B_{QCP}-B)^{0.43}$. Black solid line is a guide to the eye. Inset: logarithmic plot of T_N as a function of the reduced field $b=(B_{QCP}-B)/B_{QCP}$, where $B_{QCP}=1.23$ T. Dashed green line is $T_N(b) \propto b^{0.43}$. (b) $M(B)$, normalized to $M_S=M(4 T)=1.7 \mu_B/\text{Yb}$ for $T=0.06$ K. Plateaux in M/M_S correspond to peaks in the inverse susceptibility $1/(dM/dB)$ (dashed line). Inset: the Zeeman splitting of the singlet and triplet energy levels deduced from fits (see text).

indicates that the singlet and triplet dimer states have become degenerate. In dimer systems like TlCuCl_3 [43] and $\text{BaCuSi}_2\text{O}_6$ [40], this gapless and magnetic state is unstable to AF order, and T_N increases as field increases the population of dimer triplets, analogous to BEC. In $\text{Yb}_2\text{Pt}_2\text{Pb}$, the $B=0$ AF phase has already vanished when $\Delta \rightarrow 0$, although it is possible that re-entrant AF order or another collective state may result for $B \geq B_\Delta$ [44]. If such a phase emerges in $\text{Yb}_2\text{Pt}_2\text{Pb}$ above 1.2 T, the nonzero value of Δ implies that, like the $B=0$ AF phase, it too must emerge from a SL with both singlet and triplet dimers.

Perhaps the most striking signature of the SSL is the observation of quantized steps in $M(B)$, present in the field-induced AF phase in $\text{SrCu}_2(\text{BO}_3)_2$ [2, 45], and in the $B=0$ AF phase of the RB_4 [46, 47]. Here, magnetic fields collapse the singlet-triplet gap Δ , subsequently leading to the BEC of dimer triplets that are driven through a sequence of ordered superstructures of singlets and triplets with quantized values of magnetization. $\text{Yb}_2\text{Pt}_2\text{Pb}$ is like the other SSL systems, as a sequence of magnetization plateaux are evident as broadened steps in $M(B)$ or sharp peaks in dM/dB , measured at $T=0.06$ K (Fig. 3b). Increasing and decreasing field sweeps are hysteretic, indicating that $\text{Yb}_2\text{Pt}_2\text{Pb}$ approaches full saturation as $M \rightarrow M_S$ via a series of intermediate phases that are separated by first order transitions, each with increasing fractions of the saturation moment. There is a weak increase

in $M(B)$ beyond the saturation field, which may suggest partial hybridization of the Yb moments with conduction electrons. As expected, Fig. 3b shows that these $M(B)$ plateaux are only observed in $\text{Yb}_2\text{Pt}_2\text{Pb}$ in the AF state with $B \leq B_{QCP}$. Unlike $\text{SrCu}_2(\text{BO}_3)_2$, TlCuCl_3 , and $\text{BaCuSi}_2\text{O}_6$, where very large fields are required to approach saturation, in $\text{Yb}_2\text{Pt}_2\text{Pb}$ $M/M_S \rightarrow 1$ for $B \simeq 4 T$, so it is straightforward to observe the entire magnetization process.

Our experiments on $\text{Yb}_2\text{Pt}_2\text{Pb}$ provide new insight into AF order on the SSL. $\text{Yb}_2\text{Pt}_2\text{Pb}$ is a conventional paramagnet when $k_B T \gg J, J'$, but an increasing number of Yb moments form long-lived dimers as $k_B T$ decreases towards $\Delta = 4.6 K$. The stabilization of AF order requires a substantial occupancy of the excited moment-bearing triplet state, which is only possible when $k_B T_N$ is not much smaller than Δ . $\text{Yb}_2\text{Pt}_2\text{Pb}$ is the only known SSL system where this condition is met, and the apparent persistence of the singlet-triplet gap into the AF state suggests that AF order involves locking strongly bonded dimers together via weaker interdimer bonds. The phase diagram in Fig. 3a indicates that increasing either temperature or magnetic field breaks these fragile interdimer bonds, and $\text{Yb}_2\text{Pt}_2\text{Pb}$ reverts to a liquid of uncoordinated dimers.

The unique characteristics of $\text{Yb}_2\text{Pt}_2\text{Pb}$ are highlighted by comparing its properties to other SSL systems (Table 1). In the RB_4 compounds the Weiss temperature for fields in the SSL plane θ_{ab} and T_N are much larger than J and J' , and so these are conventional AFs. AF order is avoided above $T_N = 2.02 K$ in $\text{Yb}_2\text{Pt}_2\text{Pb}$, possibly due to strong single-ion anisotropy, weak Rudermann-Kittel-Kasuya-Yosida (RKKY) interactions, or to its quasi-two dimensional magnetic character, absent in the other SSL compounds. Since $k_B T_N \simeq J, J'$, competition between dimer formation and AF order is an integral feature of $\text{Yb}_2\text{Pt}_2\text{Pb}$, which can be considered the AF counterpart of the SL $\text{SrCu}_2(\text{BO}_3)_2$. As such, it is the only SSL system known so far where the interplay of dimer formation and long-ranged AF order can be studied together.

The $B=0$ ground state for $\text{Yb}_2\text{Pt}_2\text{Pb}$ is distinct among both HF and SSL compounds, with AF order developing from a liquid of dimers. The small values of the Néel temperature and the exchange interactions, as well as the suppression of AF order in a small magnetic field place $\text{Yb}_2\text{Pt}_2\text{Pb}$ very close to the AF-SL transition, a regime of the SSL that was previously only addressed theoretically. While there are other HFs that form on frustrated lattices [18], in these cases it is generally found that long ranged interactions replace the competing short ranged interactions that lead to frustration effects in insulating systems. Given that $\text{Yb}_2\text{Pt}_2\text{Pb}$ is an excellent metal with substantial Yb moments, it is noteworthy that we observe the singlet-triplet gap, the dimer SL, and the magnetization plateaux, all signatures of the SSL that were previously only observed in insulat-

ing $\text{SrCu}_2(\text{BO}_3)_2$.

TABLE I: A comparison of the Néel temperature T_N , in-plane Weiss temperature θ_{ab} , frustration figure of merit $f = \theta_{ab}/T_N$, interdimer exchange J' , intradimer exchange J , J'/J , and susceptibility anisotropy $\% = \chi_{ab}/\chi_c$, evaluated at T_N in different SSL systems (2 K for $\text{SrCu}_2(\text{BO}_3)_2$, 250 K and 30 K, respectively, for TmB_4). For $\text{Yb}_2\text{Pt}_2\text{Pb}$, θ_{ab} taken from Curie-Weiss fit of $\chi(T)$ for $20 K \leq R \leq 80 K$, where only the ground doublet of the crystal electric field manifold is appreciably occupied. T_N , θ_{ab} , J' , and J are all given in units of K.

	T_N	θ_{ab}	f	J	J'	J'/J	$\%$	REF.
$\text{Yb}_2\text{Pt}_2\text{Pb}$	2.02	8.5	4	2.3	1.9	0.83	30	This work
GdB_4	42	-68	1.6	8.9	0.68	0.076	1.05	[49–51]
TmB_4	10	-63	6.3	0.85	0.3	0.36	1.5, 20	[7]
TbB_4	44	-27	0.6	1.55	0.33	0.21	0.88	[47, 49, 52]
$\text{SrCu}_2(\text{BO}_3)_2$	–	-103	–	85	54	0.64	1.28	[3, 53]

Is heavy fermion physics important in $\text{Yb}_2\text{Pt}_2\text{Pb}$? The large value of the $B=0$ Sommerfeld constant $\gamma = C/T = 311 \text{ mJ/molK}^2$ in the AF state [32] is reminiscent of the enhanced Fermi liquid properties found in unfrustrated HF compounds located near magnetic QCPS [56, 57]. Strong fluctuations due to the magnetic frustration of the SSL are not by themselves enough to explain such large values of γ , since they are absent in the RB_4 compounds based on the classical moments $R = \text{Dy, Gd, Tm, Er, Ho}$, where Kondo physics plays no role [54, 55]. Our measurement of $\gamma = C(B)/T$ for $T = 0.25 K$ (Fig. 4) confirms that the emergence of an AF state with large γ from either a weakly interacting Fermi liquid for $B \geq 3 T$ with $\gamma \simeq 100 \text{ mJ/mol-YbK}^2$, or from the $\gamma = 30 \text{ mJ/mol-YbK}^2$ state found for $B=0$ and $T \geq T_N$, is accompanied by a strong enhancement of the quasiparticle mass, similar to what is found in field-tuned HF compounds like CeNi_2Ge_2 and YbRh_2Si_2 [56]. Sharp peaks in γ mark the suppression of the $B=0$ AF order at $1.3 T$, and the disappearance of partial order at $2.3 T$, although γ remains large throughout the field-tuned AF phase in $\text{Yb}_2\text{Pt}_2\text{Pb}$.

Our measurements show that $\text{Yb}_2\text{Pt}_2\text{Pb}$ is a very unusual system. Does the HF character of $\text{Yb}_2\text{Pt}_2\text{Pb}$ presage an incipient breakdown of normal metallic behavior and the stabilization of unconventional ordered phases that are found near AF quantum critical points in unfrustrated HF compounds, or do frustrated HF compounds have inherently different properties? $\text{Yb}_2\text{Pt}_2\text{Pb}$ is one of a very small number of known compounds where these intriguing questions can be experimentally explored.

The authors thank J. Sereni and M. Jaime for enlightening discussions. This work was supported by National Science Foundation grant NSF-DMR-0907457. After this paper was submitted, we became aware of a recent publication [58] that also reports the field and temperature dependent magnetization and specific heat of $\text{Yb}_2\text{Pt}_2\text{Pb}$.

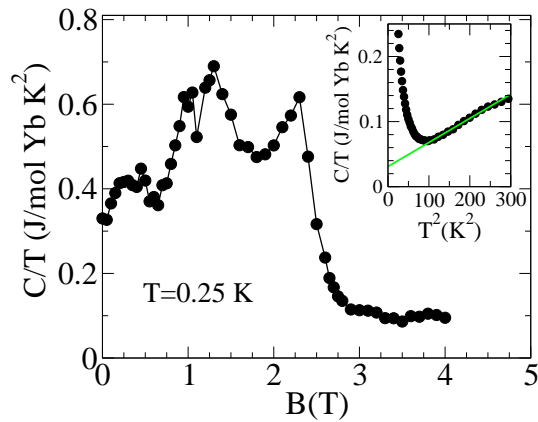


FIG. 4: (Color online) The field dependence of C/T for fixed $T=0.25$ K. This temperature was selected to ensure a minimal nuclear Schottky contribution, evident at lower temperatures. Inset: the fit (green line) to the specific heat C/T vs T^2 gives a Sommerfeld coefficient $\gamma=30$ mJ/mol Yb K^2 for the $B=0$ paramagnetic state.

-
- [1] B. S. Shastry and B. Sutherland, *Physica B* **108**, 1069 (1981).
- [2] H. Kageyama, et al., *Phys. Rev. Lett.* **82**, 3168 (1999).
- [3] S. Miyahara and K. Ueda, *J. Phys.: Cond. Matt.* **15**, R327 (2003).
- [4] K. Onizuka, et al., *J. Phys. Soc. Japan* **69**, 1016 (2000).
- [5] J. Etourneau, et al., *J. Less-Common Met.* **67**, 531 (1979).
- [6] S. Michimura, et al., *Physica B* **378 – 380**, 596 (2006).
- [7] S. Mafaš, et al., *J. Phys.: Conf. Ser.* **200**, 032041 (2010).
- [8] F. Iga, et al., *J. Magn. Magn. Mater.* **310**, e443 (2007).
- [9] Z. Weihong, et al., *Phys. Rev. B* **60**, 6608 (1999).
- [10] M. Al Hajj and J. -P. Malrieu, *Phys. Rev. B* **72**, 094436 (2005)
- [11] A. Isacsson and O. F. Syljuåsen, *Phys. Rev. E* **74**, 026701 (2006).
- [12] D. Carpentier and L. Balents, *Phys. Rev. B* **65**, 024427 (2002).
- [13] M. Albrecht and F. Mila, *Europhys. Lett.* **34**, 145 (1996).
- [14] A. Koga, et al., *J. Phys. Soc. Japan* **72**, 938 (2003).
- [15] Q. M. Si, *Phys. Stat. Sol.* **247**, 476 (2010).
- [16] P. Coleman and A. H. Nevidomskyy, *J. Low Temp. Phys.* **161**, 182 (2010).
- [17] M. Vojta, *Phys. Rev. B* **78**, 125109 (2008).
- [18] C. Lacroix, *Physica B* **404**, 3038 (2009).
- [19] M. C. Aronson, et al., *J. Low Temp. Phys.* **161**, 98 (2010).
- [20] B. H. Bernard, et al., *Phys. Rev. B* **83**, 214427 (2011).
- [21] G. R. Stewart, *Rev. Mod. Phys.* **73**, 797(2001).
- [22] H. v. Lohneysen, et al., *Rev. Mod. Phys.* **79**, 1015 (2007).
- [23] P. Gegenwart, et al., *Nature Physics* **4**, 186 (2008).
- [24] S. Paschen, et al., *Nature* **432**, 881 (2004).
- [25] S. Friedemann, et al., *Nature* **5**, 465 (2009).
- [26] S. Friedemann, et al., *J. Low Temp. Phys.* **161**, 67 (2010).
- [27] H. Shishido, et al., *J. Phys. Soc. Japan* **74**, 1103 (2005).
- [28] T. Park, et al., *Proc. Nat. Acad. Sci.* **105**, 6825 (2008).
- [29] J. G. Sereni, et al., *Phys. Rev. B* **80**, 024428 (2009).
- [30] E. Bauer, et al., *J. Optoelectron. Adv. Mater.* **10**, 1633 (2008).
- [31] E. Kikuchi, et al., *J. Phys. Soc. Japan* **78**, 083708 (2009).
- [32] M. S. Kim, et al., *Phys. Rev. B* **77**, 144425 (2008).
- [33] L. S. Wu, et al., *Phys. Rev. B* **84**, 134409 (2011).
- [34] A. P. Ramirez, *Ann. Rev. Mat. Sci.* **24**, 453 (1994).
- [35] Y. Sasago, et al., *Phys. Rev. B* **52**, 3533 (1995).
- [36] R. W. Reynolds et al., *J. Chem. Phys.* **56**, 5607 (1972).
- [37] N. Kawashima, *J. Phys. Soc. Japan* **73**, 3219 (2004).
- [38] P. Gegenwart, et al., *Science* **315**, 969 (2007).
- [39] T. Park, et al., *Nature* **440**, 63 (2006).
- [40] S. E. Sebastian, et al., *Nature* **441**, 617 (2006).
- [41] F. Yamada, et al., *J. Phys. Soc. Japan* **77**, 013701 (2008).
- [42] T. Giamarchi, et al., *Nature Physics* **4**, 196 (2008).
- [43] C. Rugg, et al., *Nature* **423**, 62 (2003).
- [44] Y. Yoshida, et al., *J. Phys. Soc. Japan* **74**, 2917 (2005).
- [45] S. E. Sebastian, et al., *Proc. Nat. Acad. Sci.* **105**, 20157 (2008).
- [46] K. Siemensmeyer, et al., *Phys. Rev. Lett.* **101**, 177201 (2008).
- [47] S. Yoshii, et al., *Phys. Rev. Lett.* **101**, 087202 (2008).
- [48] J. Rossat-Mignot et al., *J. Magn. Magn. Mater.* **31 – 34**, 398 (1983).
- [49] Z. Fisk, et al., *Sol. St. Comm.* **39**, 1189(1981).
- [50] J. Fernandez-Rodriguez, et al., *Phys. Rev. B* **72**, 052407 (2005).
- [51] A. Kikkawa, et al., *J. Phys. Soc. Japan* **76**, 024711 (2007).
- [52] J.-S. Rhyee, et al., *J. Appl. Phys.* **101**, 09D509 (2007).
- [53] H. Kageyama, et al., *J. Phys. Soc. Japan* **68**, 1821 (1999).
- [54] R. Watanuki, et al., *J. Phys. Soc. Japan* **74**, 2169 (2005).
- [55] V. V. Novikov, et al., *J. Appl. Phys.* **111**, 063907 (2012).
- [56] R. Kuchler, et al., *Phys. Rev. Lett.* **91**, 066405 (2003).
- [57] H. v. Lohneysen, et al., *Rev. Mod. Phys.* **79**, 1015 (2007).
- [58] A. Ochiai, et al., *J. Phys. Soc. Japan* **80**, 123705 (2011).